Hindawi
Advances in Polymer Technology
Volume 2019, Article ID 2707616, 14 pages
https://doi.org/10.1155/2019/2707616

Research Article

The Characteristics of Oil Occurrence and Long-Distance Transportation due to Injected Fluid in Tight Oil Reservoirs

Liu Yang,[1] Jun Yang ,[1] Jian Gao,[2] and Xuhui Zhang[3]

[1]*State Key Laboratory for Geomechanics and Deep Underground Engineering, China University of Mining and Technology (Beijing), Beijing 100083, China*
[2]*Research Institute of Petroleum Exploration and Development, Beijing 100083, China*
[3]*Key Laboratory for Mechanics in Fluid Solid Coupling Systems, Institute of Mechanics, Chinese Academy of Sciences, Beijing 100190, China*

Correspondence should be addressed to Jun Yang; yjlr@163.com

Received 21 March 2019; Revised 23 July 2019; Accepted 8 August 2019; Published 1 December 2019

Guest Editor: Fang Hu

In tight oil reservoirs, the injected fluid needs to travel a long distance to expel oil from the micro/nano-size pores to natural fractures or man-made fractures. The flow characteristics of injected fluid are not known well due to the long distance displacement and complex pore structure. In this study, the tight reservoir samples are from typical tight oilfield of China and the oil distribution characteristics are studied based on mineral composition, physical properties and pore size distribution. The long core displacement experiment is conducted based on injection of water, N_2, and CO_2, which aims to study the individual flooding feasibility. The results show that the oil mainly distributes in the form of spots and accumulates in the micro/nano-pores. Both oil spots and clay minerals have associated characteristics. The microfractures are not the storage space for oil spots, but can connect the oil spots to improve the mobility of the crude oil. In addition, the oil can achieve long distance migration under the injection of water, N_2, and CO_2, which presents different pressure distribution characteristics. The reservoir pressure of water flooding decreases first and increases later with displacement time. The reservoir pressure of N_2 flooding rises gradually over displacement time. The reservoir pressure of CO_2 flooding increases first and decreases over displacement time. In contrast to water flooding, N_2, and CO_2 can increase the reservoir energy, which contributes to tight oil production. In comparison, CO_2 has better performances than N_2 in terms of oil displacement efficiency. The study contributes to understanding the oil distribution characteristics and provides the guidance for field trials using different flooding techniques.

1. Introduction

The tight oil, significant hydrocarbon resources, has recently become a hot topic for exploration and development following shale gas [1]. Tight oil reservoirs are characterized by ultralow permeability, which obstructs hydrocarbons flow to wellbores without stimulation [2]. Horizontal-well drilling and multistage fracturing are the effective and economic technology for the exploitation of oil and gas [3]. Although the production is encouraging, intractable problems are also apparent. One of the problems is the fast decline of production in individual producers during depletion development, forcing operators to refracture existing wells or drill new wells [4]. In order to maintain the production rate, it is essential to establish efficient flooding systems for reservoir energy supplement and enhancing oil recovery [5].

In contrast to conventional sandstone, limestone, and carbonate reservoirs, tight oil reservoirs have much lower permeability (<1 mD) and more complicated pore structure [6]. The pore size and connectivity of tight oil reservoirs are greatly less than that of conventional reservoirs [7]. The crude oil tends to be entrapped in small pores, suggesting natural inability of oil flow in tight oil reservoirs [8, 9]. Although water flooding has been widely used to improve oil production in conventional reservoirs, it is difficult to apply these technologies for unconventional reservoirs due to high capillary pressure and low injectivity [10]. Lots of experimental studies have been performed to promote the oil transportability in tight oil reservoirs, including water imbibition, N_2 injection and carbon dioxide extraction [11, 12]. However, the experiments were conducted in low-temperature and low-pressure conditions that cannot represent actual reservoirs. In addition, few studies

Table 1: The basic properties of formation water.

Cation, mg/L			Anion, mg/L			PH	Total salinity, mg/L	Density, g/cm^3	Type
Na^++K^+	Ca^{2+}	Mg^{2+}	Cl^-	SO_4^{2-}	HCO_3^-				
3621	1782	12	7831	8	1300	6.0	14321	1.013	$CaCl_2$

involve fluid properties or the experimental tests are carried out on fluids of simple composition (e.g., kerosene and mineral oil). In the future investigation, these technologies should be evaluated under representative reservoir conditions [13].

CO_2 injection technology has been successfully applied in many oilfields, including conventional oil reservoirs and low-permeability reservoirs. The field studies show that recovery efficiency can be larger than 60% in some oil fields [14, 15]. CO_2 can recover oil by reducing residual oil saturation, interfacial tension, and oil viscosity [16]. Teramoto et al. [17] pointed out that the technology is more feasible at high water-cut stage during the development of light oil reservoir. However, the sweep efficiency is limited in many fractured reservoirs because CO_2 can directly flow though fractures due to instabilities in the gas viscosity [18]. CO_2 huff and puff is used to mitigate these drawbacks in this circumstance [19]. The same well involves both producing oil and injecting gas, and the fractures tend to help extend the exposure area influenced by CO_2 [20]. Previous research found that the viscous flow is seriously restricted because of high capillary resistance and diffusion may be the primary mechanism for oil transport and recovery in tight oil reservoirs [21]. As for CO_2 enhanced oil recovery, the improvement of diffusion-dominated oil flow is a critical oil-recovery mechanism [22]. Recent studies show that super-critical CO_2 could significantly enhance the diffusion process to improve the oil transportability in tight reservoirs [23].

Many investigations are performed on laboratory and field trials of CO_2 flooding techniques, demonstrating that it can significantly enhance oil recovery in oil reservoirs [24]. Globally, previous studies primarily focus on high and low permeability reservoirs, but little attention is paid to tight reservoirs in continental basin. Few studies report the energy supplement efficiency of different flooding systems in tight oil reservoirs by using long core displacement experiment. Chang 7 formation of Erdos Basin is the most typical and potential target for tight oil in China. The depletion drive is often used to extract small volumes of oil, which recovers only about 8-12% of oil in place. More efficient technology must be explored to mobilize a portion of the oil trapped in tiny pores. In this study, the comparative experiments of water, N_2 and carbon dioxide injection are carried out on the long cores (1 m). The pressure profiles along the length direction, enhanced oil recovery (EOR) and displacement front velocity are studied to explore the potential methods for EOR and economic production in tight oil reservoirs.

2. Experiments

The experimental materials include tight reservoir samples and fluids used for displacement tests. The basic properties of rock and fluid are shown in the following paragraph.

2.1. Fluids. The oil for rock saturation is kerosene with a viscosity of 1.3 cp and a density of 0.8 g/cm^3. N_2 and carbon dioxide gas have high purity of 99.999%, which are used as the gas source. In pursuance of real reservoir condition, formation water collected from production line is slightly yellow and used for this experiment. Instead of distilled water, formation water is essential to minimize the effects of water sensitivity. Table 1 presents the basic properties of formation water. The cleaning fluids include toluene, methylene chloride and methanol, which are used to remove the oil in tight reservoirs samples.

2.2. Tight Rock Samples

2.2.1. Mineral Composition. The cores of tight oil reservoirs are taken from the outcrop of Chang 7 formation in Ordos Basin. The lithology is primarily characterized by fine-grained sandstone and siltstone. The tight oil formation has a large potential for future oil exploration and development. According to the mineralogy composition analysis, the outcrop sample is characterized by low concentration of clay (11.4%) and high concentration of quartz (44%) and feldspar (32%) (Figure 1(a)). The ilite and I/S (illite/smectite mixed-layer) are the primary clay minerals. The tight oil reservoirs may not be seriously sensitive to water due to low content of clay minerals.

2.2.2. Physical Properties. The displacement experiment requires cuboid shape sample with 4.5 cm wide, 4.5 cm high and 100 cm long (Figure 2). Conventional sandstone with high porosity and permeability is used as a calibration standard. For tight oil reservoirs, the porosity is estimated to be about 10.5–11.8% and the permeability ranges 0.6 mD to 1.7 mD (Table 2). The tight rock samples are weighted, vacuumed, saturated with formation water and weighed again. Then the porosity is determined using the density of formation water. In addition, the samples are flooded with formation water at the steady state condition. The flow rate and core holder inlet-outlet pressure difference are measured. Then the permeability is determined based on the Darcy's equation.

2.2.3. Pore Structure. The scanning electron microscopy (SEM) can help explore the pore structure of tight rocks at the micro/nano-scales. The presence of complex pores is confirmed by SEM (Figure 3). Both microfractures and matrix pores are well developed in the samples. The microfractures present high connectivity and can connect to matrix pores and other microfractures. To some extent, the presence of microfractures enhances the sample permeability. In addition, the most common pores have the pore diameter of 0.8–3.6 μm, most of which are irregular polygon-shaped and have poor connectivity.

The pore size distribution is obtained by mercury intrusion and nuclear magnetic resonance (NMR) test, as shown

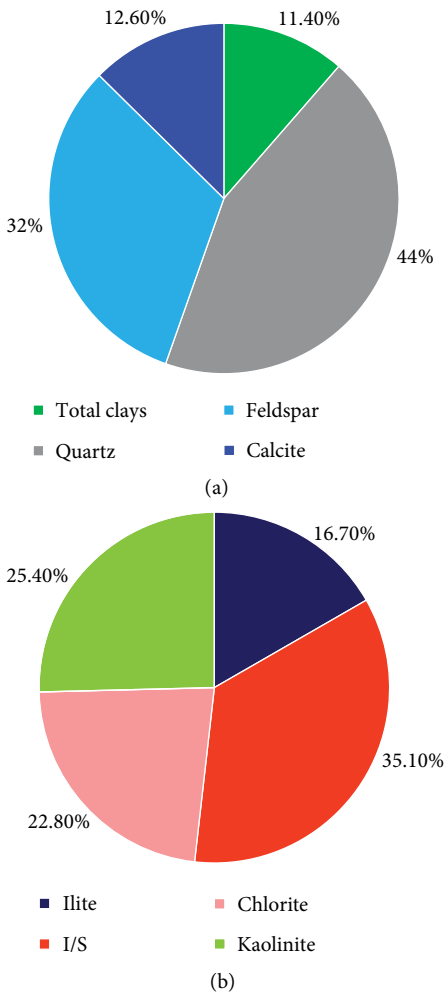

Figure 1: The mineralogy composition of samples: (a) bulk mineral composition, (b) clay mineral composition.

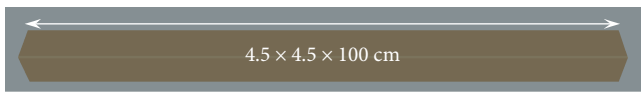

Figure 2: The outcrop sample for long core displacement experiments.

Table 2: The physical properties of tight reservoirs samples.

Sample	Formation	Porosity, %	Permeability, mD
Conventional sandstone (water injection)	--	20.2	1414
Sample 1# (water injection)	Chang-7	10.5	0.6
Sample 2# (N_2 injection)		11.3	1.2
Sample 3# (CO_2 injection)		11.8	1.7

in Figure 4. The NMR apparatus (MiniMR-VTP) is made by Suzhou Niumag Analytical Instrument Corporation. The NMR T_2 spectra agree well with the mercury intrusion results.

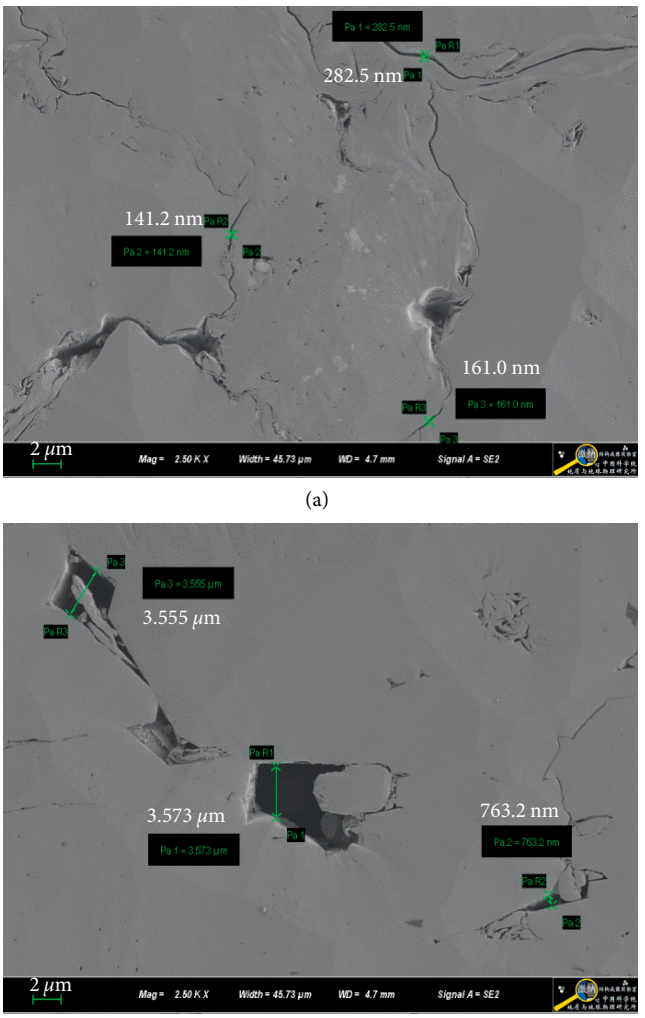

Figure 3: The SEM of tight oil reservoir samples.

The dual-peak distribution characteristics indicates the development of microfractures and matrix pores. The left peak mainly reflects the characteristics of the matrix pores with the pore size of lower than 1.0 μm. In addition, the pore volume of the left peak accounts for more than 90% of the total pore volume. Combined with the results of NMR and mercury intrusion, the surface relaxivity of 50 nm/ms can be calculated.

2.2.4. Oil Distribution Characteristics. Studying the distribution characteristics of tight oil is of great significance for exploring the "sweet spot" and understanding the enrichment pattern. The downhole core samples are also taken from the Chang-7 formation at a depth of 2300 m that is consistent with the formation of outcrop sample used in the experiment. After removing the core from the bottom of the well, it is immediately sealed to prevent oil and gas from escaping. According to the SEM observation standard, the surface of the sample is polished by argon ion and the oil distribution characteristics is observed, as shown in Figure 5. Both matrix pores and microfractures are well developed in the tight reservoirs. It is necessary to separately

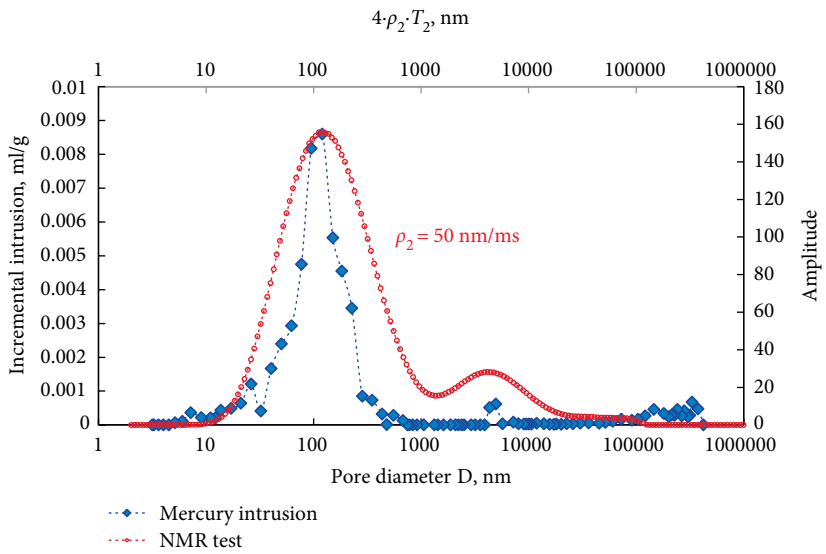

Figure 4: The pore size distribution by mercury intrusion and NMR test.

study the effects of pores and microfractures on the distribution of tight oil.

The SEM results show that the oil spots in matrix pores present sporadic distribution and poor continuity (Figure 5). Clay minerals are often developed in oil-spot aggregation areas, suggesting the certain associated characteristics of oil and clay minerals. According to the mineralogy composition of Figure 1, the clay minerals include ilite, I/S, chlorite and kaolinite. It should be noted that clay minerals type may have an important influence on the enrichment pattern and migration of tight oil.

The microfractures of different scales are widely developed and distributed in a network. Figure 6 presents the oil distribution characteristics in microfractures. It can be seen that most of the microfractures are not filled with oil. It suggests that microfractures are not the main space for oil distribution, which largely limits the oil production. However, some microfractures can penetrate the oil spots and connect the oil spots with sporadic distribution, which will greatly improve the mobility of the crude oil.

2.3. Experimental Setup. The one-dimensional core displacement apparatus is often used for different flooding experiments. In this study, the long displacement apparatus (1 m long) is designed to explore the pressure profile in the tight reservoirs. The displacement apparatus includes injection system and displacement system (Figure 7). The injection system is mainly composed of ISCO pump, brine/injected gas and other components. The displacement system is made up of pressure sensors, long core holder, measuring bottle and back-pressure valves.

The pressure sensors can facilitate the pressure identification during all kinds of flooding. Nine pressure transducers are installed at the intervals of about 12.5 cm to monitor the real-time changes of pressure profile along the length direction. The displacement pressure is 25 MPa, back-pressure is 5 MPa, and confining pressure is 32 MPa. The test temperature is 25°C. The back-pressure valve is utilized on the outlet to simulate constant pressure during production (Figure 7).

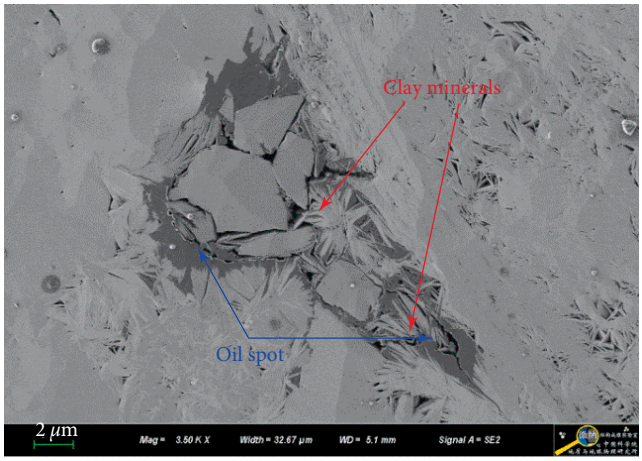

(a)

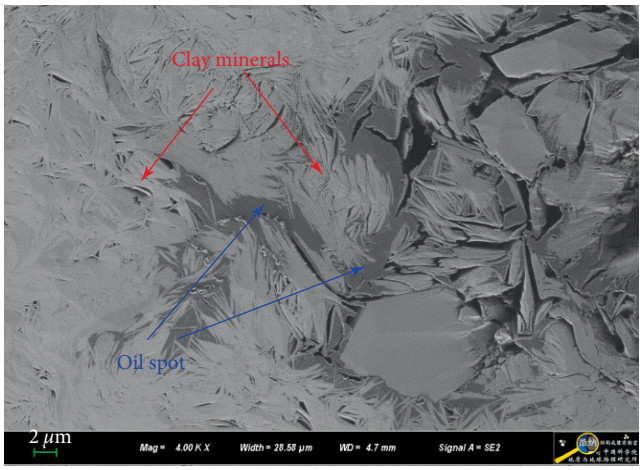

(b)

Figure 5: The oil distribution characteristics in matrix pores.

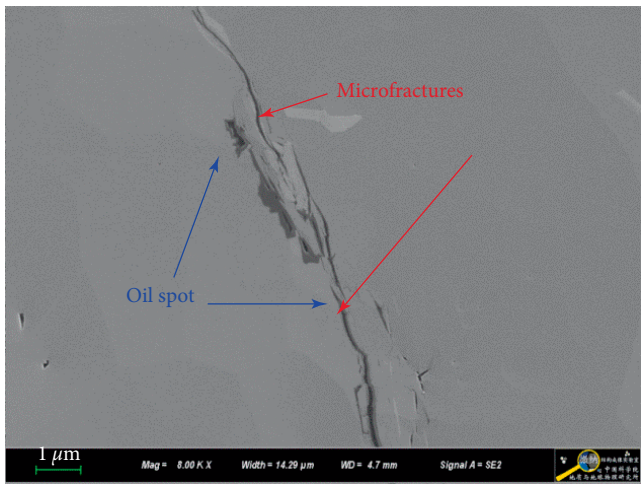

(a)

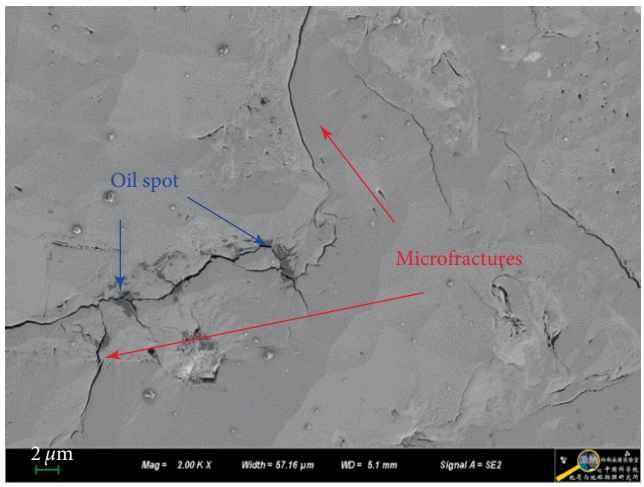

(b)

Figure 6: The oil distribution characteristics in microfractures.

2.4. Experimental Preparation and Procedures. The experimental preparation is as follows:

(1) Each cuboid samples are washed thoroughly using cleaning fluids and dried at the temperature of 105°C to remove the moisture. The samples are put into the oven for 48 hrs and weighed very 6 hrs. If the weight error is less than 1%, the drying process is completed. The analytical balance (Mettler Toledo ME204E) is used to determine the sample mass.

(2) In order to saturate the samples with kerosene, it is necessary to use a vacuum pump to remove the air for 2 days. The tight samples are saturated with kerosene at the injection pressure of 10 MPa for 48 hrs.

(3) The saturated weight of all the samples are recorded to calculate the oil saturation of the tight rock samples.

(4) After the oil saturation processes, the samples are placed in long core holder. The injection pressure is set to 25 MPa and the back-pressure is set to 5 MPa. Only kerosene is injected to record the pressure changes along the length direction. The pressure characteristics of single phase fluid flow can act as calibration standard to study two phase fluid flow.

(5) The injection pump of kerosene is closed and the injection pump of water, N_2 or CO_2 is opened to conduct the different flooding experiments. Record the real-time changes of pressure and measure the volume of recovered oil.

3. Results and Discussions

The real-time pressure changes of long core samples are monitored during different flooding experiments (i.e., water, N_2 and CO_2 flooding). In order to benchmark the measurements, the pressure profile of conventional sandstone samples is also monitored under the same conditions. Finally, the comparative studies are conducted on displacement front speed, pressure distribution and oil displacement efficiency of water, N_2, and CO_2 flooding.

3.1. Water Flooding in Conventional Reservoirs and Tight Oil Reservoirs

3.1.1. Water Flooding in Conventional Reservoirs. The conventional sandstone sample is used to conduct water flooding experiment, which can act as a as calibration standard. The water flooding in conventional reservoirs does not need too high injection pressure. The displacement pressure is set to 5.3 MPa, back-pressure pressure is set to 5.1 MPa, and confining pressure is set to 7 MPa. The experimental results of conventional sandstone samples are presented in (Figures 8 and 9).

The experimental process includes three stages. In stage 1, only oil is injected to study the single phase fluid flow before injection time 0 min. In stage 2, the formation water pump is opened instead of oil pump and oil–water two phase flow is simulated. In stage 3, the water displacement front arrives at the outlet. At the injection time 125 min, the formation water is found in measuring bottle, suggesting that two phase flow stage begins to translate into water flow stage. The water breakthrough time is about 125 min.

Figure 8 presents the pressure change along the flow direction over injection time. In spite of three stages, the pressure curves are approximately horizontal and parallel. No pressure fluctuation is observed during water flooding, suggesting that water flooding front has little impact on fluid pressure in conventional reservoirs. Figure 9 indicates the pressure distribution along the displacement direction. The pressure P_t has a linear relationship with distance L and the pressure drop per unit distance is constant. Classically, the oil and water saturation can affect reservoir pressure by changing the relative permeability and capillary pressure. In high permeability reservoirs, there is almost no difference between oil and water permeability, and the capillary pressure is too small. Therefore, the water flooding front cannot result in reservoirs pressure fluctuation.

3.1.2. Water Flooding in Tight Oil Reservoirs. Figure 10 presents the experimental results of water flooding in the tight oil reservoirs. A significant difference is detected between

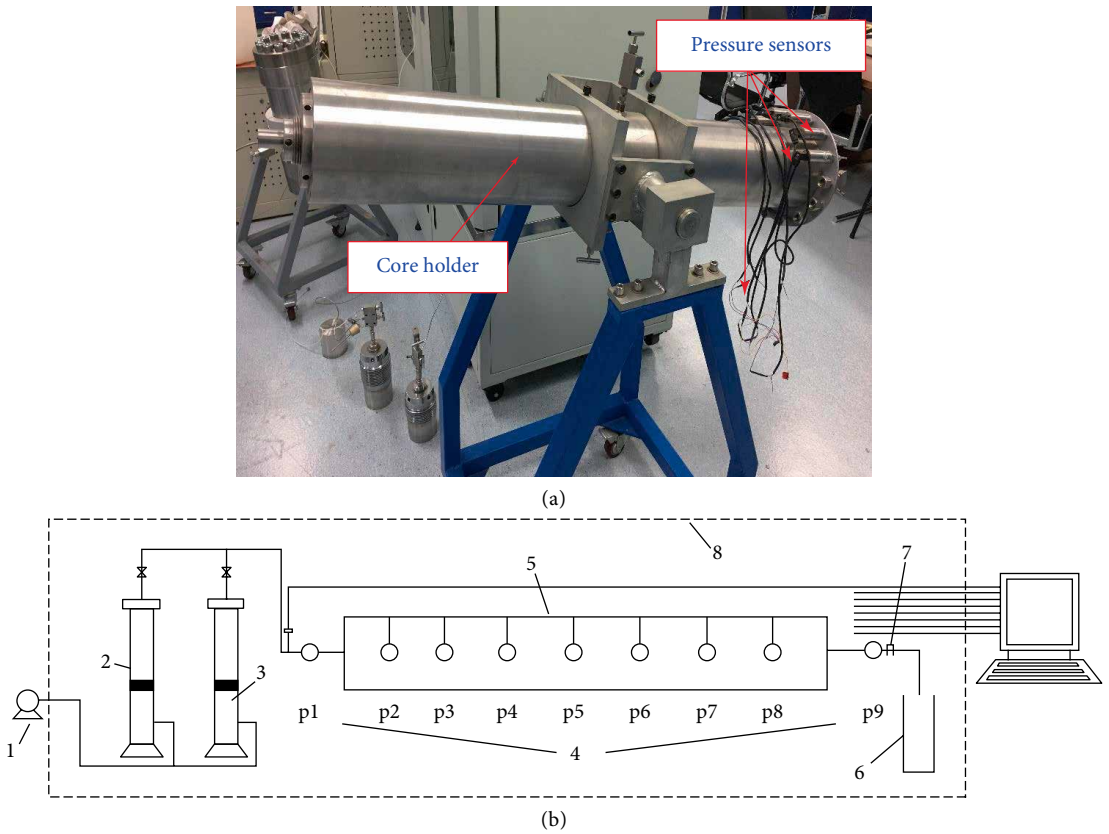

Figure 7: Schematic illustration of long core flooding apparatus. 1: ISCO pump; 2: brine/injected gas; 3: simulated crude oil; 4: pressure transducers; 5: core holder; 6: measuring bottle; 7: back-pressure valves; 8: oven.

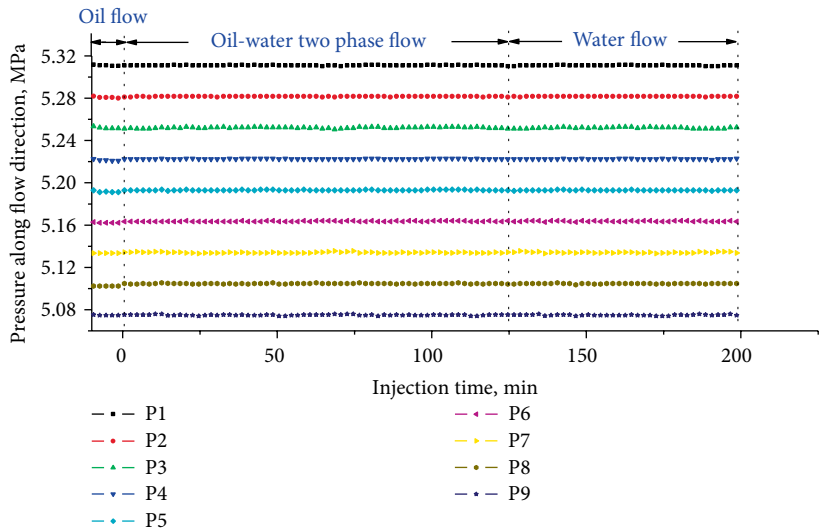

Figure 8: The relationship between pressure along flow direction and injection time in conventional sandstone reservoirs. The P1–P9 indicates the pressure at different locations of samples.

conventional reservoirs and tight oil reservoirs. For tight oil reservoirs, there is significant pressure fluctuation during water flooding. The 7 valley "V" curves are found in the stage of oil-water two phase flow. The pressures of P1 and P9 are always constant, which are 25 MPa and 5 MPa respectively. However, the pressures of P2 to P8 firstly decrease and then increase over time. The pressure curves schematic of monitoring points (P2-P8) are presented in Figure 11. The pressure decreases to "valley bottom" in the left side and the pressure increase from "valley bottom" in the right side. There is a common feature between the left and right side that the rate of pressure change gradually slows down.

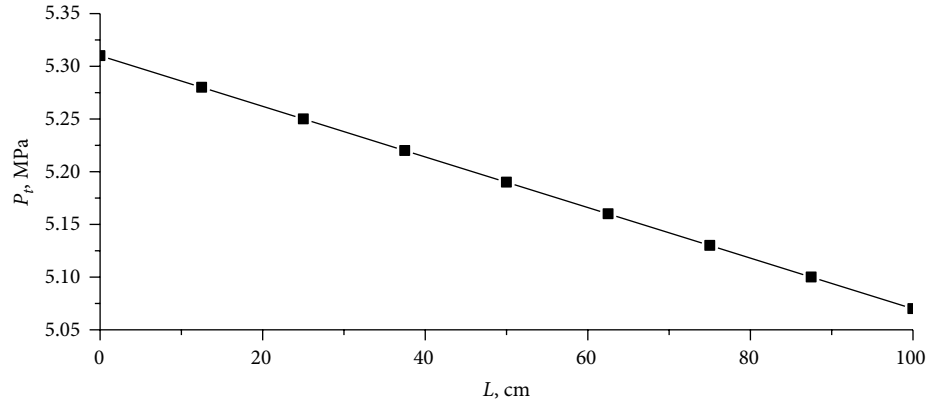

Figure 9: The pressure distribution along the displacement direction in conventional sandstone samples.

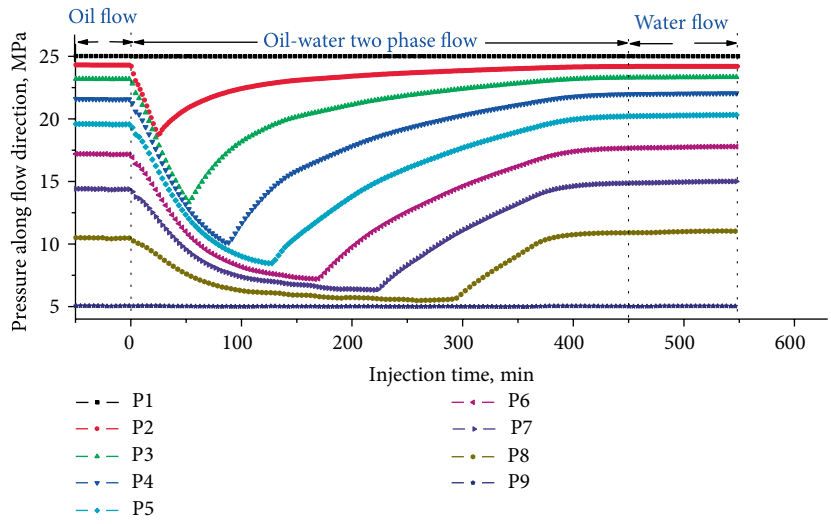

Figure 10: The water flooding results in tight oil reservoirs.

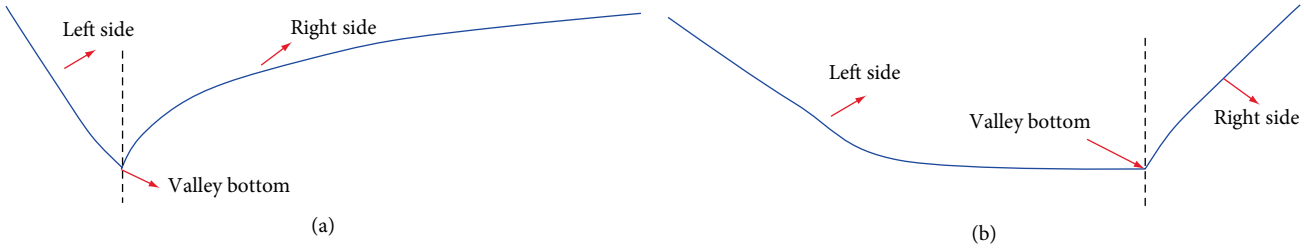

Figure 11: Pressure curves schematic of monitoring points (P2–P8): (a) P2–P6 and (b) P7-P8.

In the stage of oil-water two phase flow, the pressure fluctuation reflects the oil–water distribution change. In the tight oil reservoirs, the water saturation can change the relative permeability and capillary pressure, which can affect the displacement pressure. The pore diameter is about 0.1 μm in tight oil reservoirs (Figure 4). It is assumed that the interfacial tension is about 0.071 N/m and the contact angle is assumed to 0°. The capillary pressure may be lower than 0.14 MPa. It seems that the capillary pressure can be neglected when compared with great displacement pressure. However, the capillary pressure is a function of water saturation. The great water saturation changes of displacement front can result in superhigh flow resistance. To some extent, it is the primary cause of low injectivity in tight reservoirs. In addition, the displacement front corresponds to the pressure decline.

Figure 12 presents the pressure distribution along the displacement direction in in tight reservoirs samples. The black curve of 0 min represents the pressure characteristics of oil flow. In contrary to the conventional sandstone with linear relationship between pressure and distance, the pressure drop is not constant and increases with distance in tight oil reservoirs. It is related to the increase of stress sensitivity as

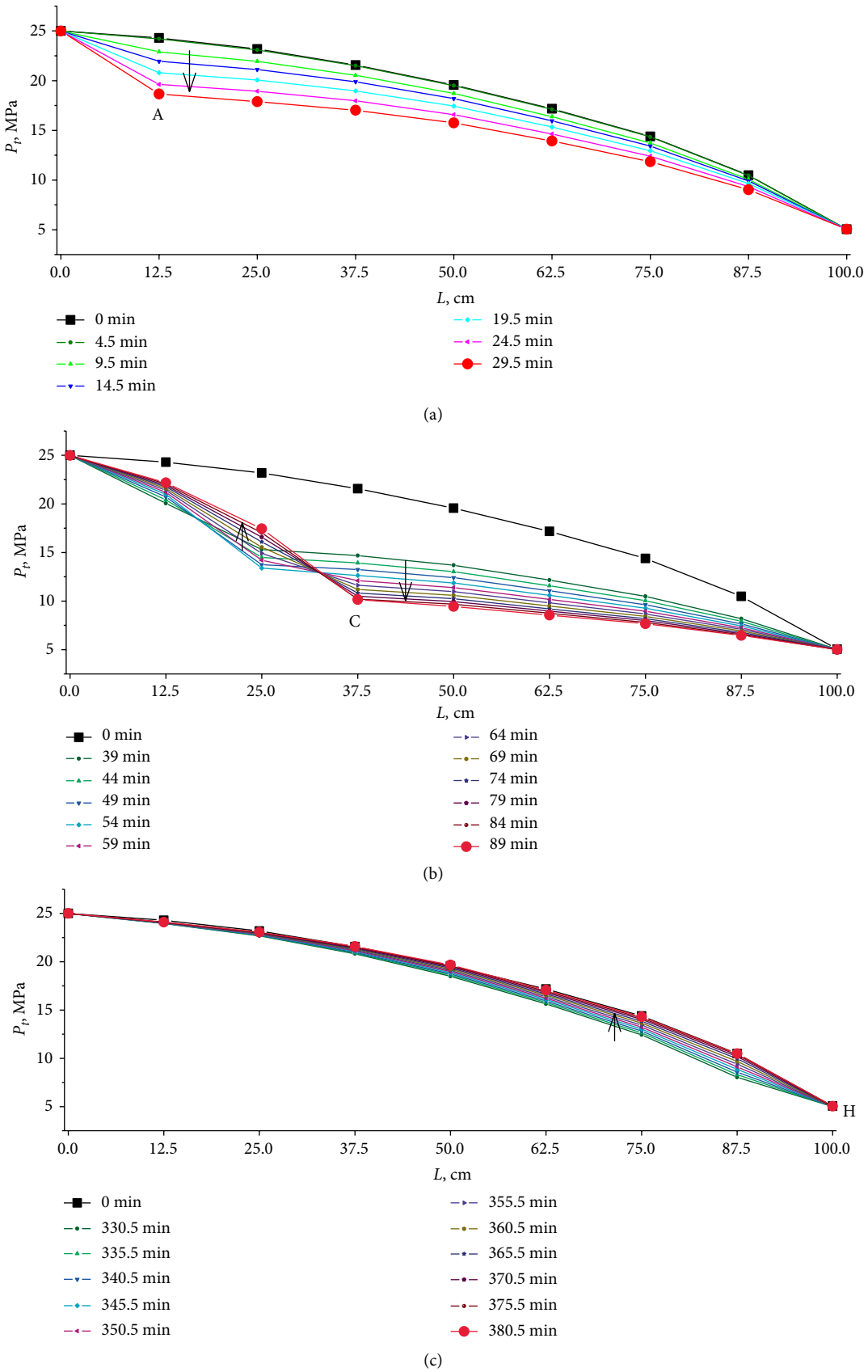

Figure 12: The pressure distribution in tight reservoirs samples during water flooding: (a) 0–29.5 min, (b) 39–89 min and (c) 330.5–380.5 min. The black curve of 0 min represents the pressure characteristics of oil flow.

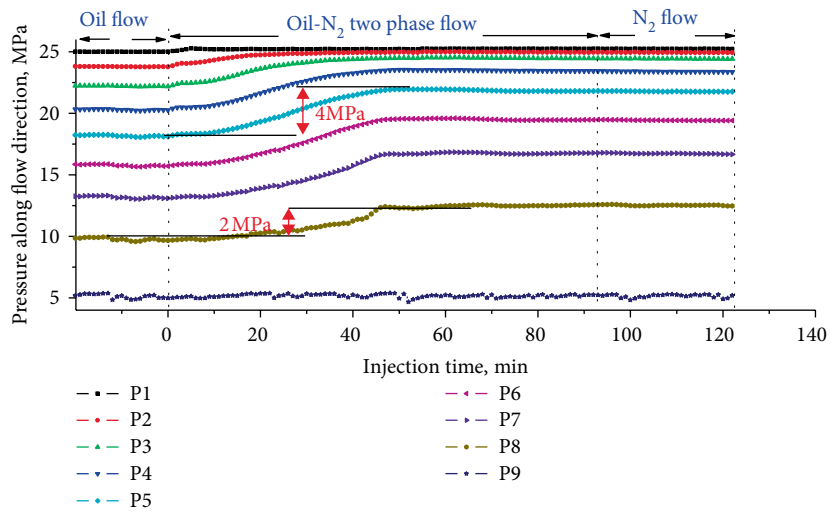

Figure 13: The N_2 flooding results in tight oil reservoirs.

distance. The pore pressure drops from 25 MPa at the inlet end to 5 MPa at the outlet end. The effective stress increases from 7 MPa at the inlet end to 27 MPa at the outlet end. Due to the stress sensitivity, the permeability samples decreases as distance, but the flow resistance of samples increases as distance, which result in non-constant pressure drop.

3.2. N_2 Immiscible Flooding in Tight Oil Reservoirs. Figure 13 presents the experimental results of N_2 flooding in tight oil reservoirs. The pressure of N_2 flow stage is much larger than that of oil flow stage. The low viscosity N_2 has much smaller flow resistance than oil. It suggests that N_2 can well maintain the reservoirs energy during flooding operations. The pressure characteristics of oil-N_2 two phase flow are different from that of oil-water two phase. The pressure increases as the injection time gradually. The significant pressure rise is accompanied by N_2 displacement front. The 7 "S" curves are found in the stage of oil-N_2 two phase flow. In the initial stage, the pressure did not change much with time. As time increases, the pressure rises rapidly. In the later stage, the pressure tends to be constant. The pressure curves are shaped like "S". The range of pressure rise due to N_2 injection is related to displacement distance L. When $L < 50$, the range of pressure rise changes gradually from 1 MPa to 4 MPa. When $L = 50$, the range of pressure rise reaches the maximum value (about 4 MPa). When $L > 50$, the range of pressure rise changes gradually from 4 MPa to 2 MPa.

The pressure distribution along the displacement direction is presented in Figure 14. As expected, N_2 flooding has better performance than water flooding. The pressure of P2–P8 has been increased to varying degrees. When the displacement time exceeds 50 min, the pressure of P2–P8 does not change anymore. Compared to water flooding, the pressure gradient at the inlet end of the N_2 flooding is significantly reduced. It shows that the N_2 flooding has a strong injection capacity. A effective displacement system can be established using N_2 injection. In addition, N_2 flooding increases reservoir pore pressure, which reduce effective stress and relieve stress sensitive damage. It contributes to long distance migration of oil. It should be noted that the interactions between N_2 and oil can reduce the interfacial tension, oil viscosity and density, which contribute to oil flow in matrix pores.

3.3. CO_2 Miscible Flooding in Tight Oil Reservoirs. Figure 15 presents the pressure profiles during the CO_2 flooding. The pressure characteristic of CO_2 flow is similar to that of N_2 flow. The pressure of CO_2 flow stage is much larger than that of oil flow stage, resulting from the low viscosity and flow resistance of CO_2. The CO_2 injection can increase the pore pressure and maintain the reservoirs energy. The 7 bell-shaped curves are demonstrated in the stage of oil-CO_2 two phase flow. The pressure gradually increases to the maximum value of "bell top" and then slowly decreases. The pressure of right side is larger than that of left side, as shown in Figure 16. From P2 to P8, the bell top gradually changes from obtuse head to acute head. It suggests that the time length of maximum value state is related to reservoir pore pressure. The higher pore pressure corresponds to larger time length of maximum value state. Unlike the flow of N_2 and water, the curve of CO_2 flow is smooth under high pressure, but it has obvious fluctuations at low pressure. The CO_2 dissolved in the water is gradually released at the low pressure, causing pressure fluctuations to some extent.

The pressure characteristics are related to the miscible displacement of CO_2. When CO_2 is injected into the reservoir, it contacts the oil in the pore, resulting in the transition zone (Figure 17). When the reservoir pressure of inlet end exceeds the minimum miscibility pressure, CO_2 begins to dissolve in kerosene substantially during the multiple contact miscible process. In the tight oil reservoirs, the transition zone changes into miscible zone. Actually, it is difficult to distinguish between transition zone and miscible zone. The CO_2 dissolution in oil can result in oil swelling, viscosity and interfacial tension reduction, which can improve the oil mobility. It plays important roles for enhanced oil recovery. From the inlet to outlet, the pressure gradually decreases from 25 MPa to 5 MPa.

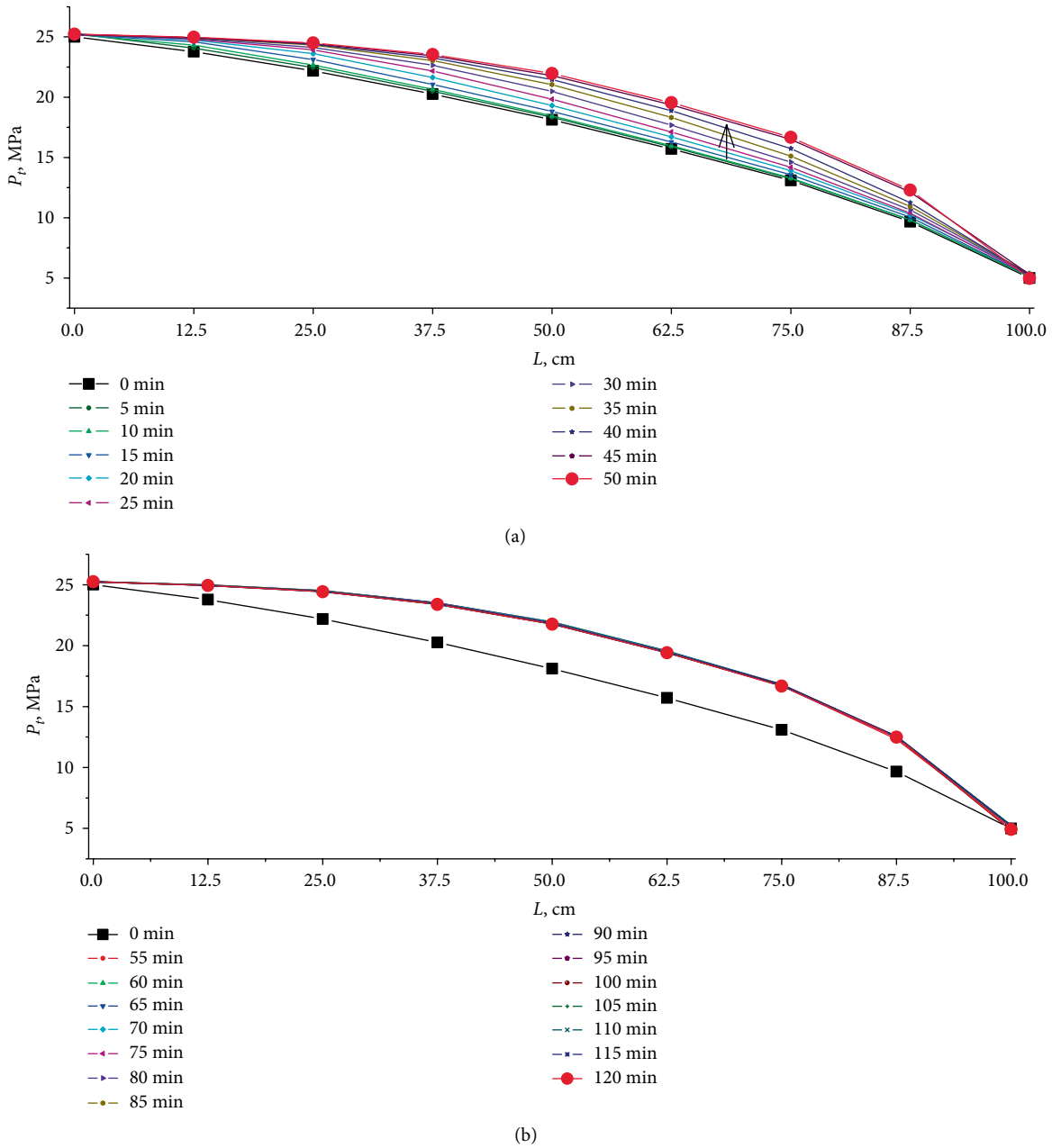

FIGURE 14: The pressure distribution in tight sandstone samples during N_2 flooding: (a) 0–50 min and (b) 55–120 min.

When the pressure is lower than minimum miscibility pressure, the miscible zone gradually decreases and even disappears completely. The oil zone and CO_2 zone begin to appear (Figure 17).

Figure 18 presents the pressure distribution along the CO_2 displacement direction. The pressure of P2–P8 increase gradually over time before 55 min. When the displacement time exceeds 55 min, the pressure of P2–P8 begins to decrease over time. When the displacement time exceeds 75 min, the pressure of P2–P8 does not change anymore. Compared with water flooding, the pressure gradient at the inlet end is significantly reduced during the CO_2 flooding, suggesting the well injection capacity of CO_2. An effective displacement system can be established for oil migration. In addition, CO_2 flooding can also increase pore pressure, reduce effective stress and relieve stress sensitive damage. An effective displacement system can be established for oil migration by CO_2 displacement.

3.4. The Comparison of Water, N_2 and CO_2 Flooding in Tight Oil Reservoirs. The water, N_2 and CO_2 flooding can improve the oil mobility and enhance oil recovery. In order to explore the suitable displacement measure for Chang 7 formation, it is necessary to carry out comparative study of water, N_2 and CO_2 flooding. The displacement front velocity, energy supplement efficiency and oil displacement efficiency are the most important parameters for evaluating flooding performance.

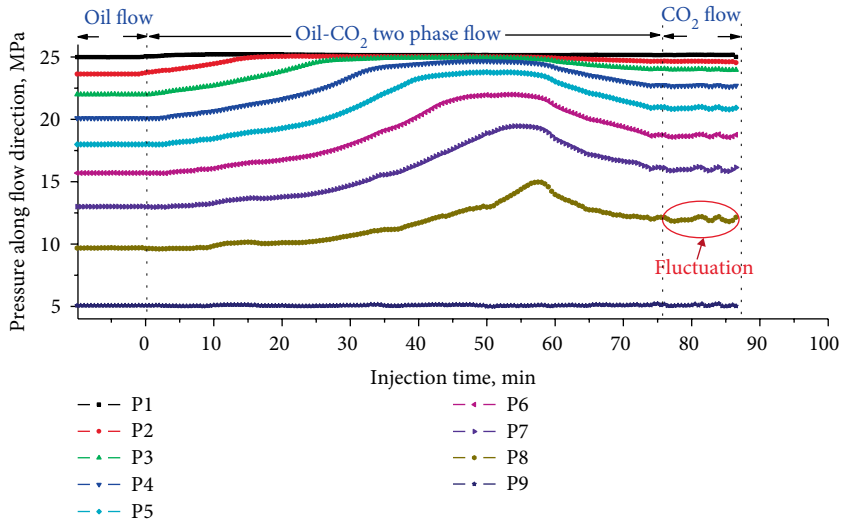

Figure 15: The CO_2 flooding results in tight oil reservoirs.

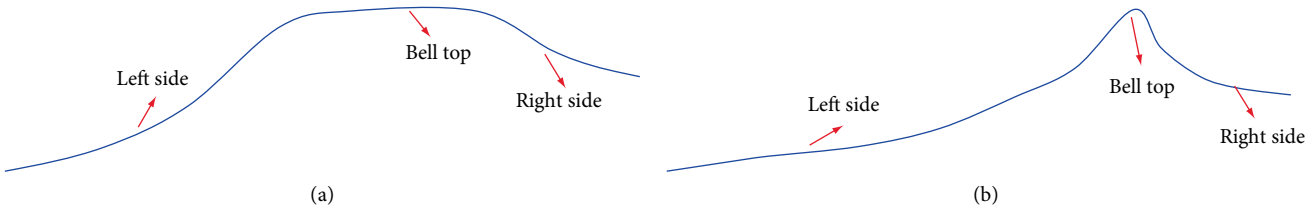

Figure 16: Pressure curves schematic of monitoring points (P2–P8): (a) P2–P6 and (b) P7-P8.

3.4.1. The Displacement Front. The water, N_2 and CO_2 injection can lead to the pressure drop or rise in the stage of two phase flow. To some extent, the pressure fluctuation indicates the movement of displacement front. Figure 19 presents the relationship between displacement front position and displacement time. During water flooding, the displacement front position is linear with time at initial stage (<180 min), but it deviates gradually from linear relationship at the late stage (Figure 19). The displacement front velocity decreases with the time, which is related to the permeability reduction induced by stress sensitivity. It takes about 400 min to get the outlets. Compared with water flooding, N_2 and CO_2 only take 55 min to reach the outlet, therefore they have higher front velocity than water flooding. Moreover, it seems that the front velocity increases over time and even tends to be infinite at the outlet. It may be related to viscous fingering. The CO_2 and N_2 have much lower viscosity than oil and may directly flow through high permeability zones, without contacting much oil in matrix pores. Compared with water flooding, CO_2 and N_2 flooding have poorer sweep efficiency. It should be noted that it is more difficult to identify the displacement front according to the pressure fluctuation characteristics of N_2 and CO_2 flooding.

3.4.2. The Energy Supplement Efficiency (ESE). A definition called energy supplement efficiency (ESE) is used in order to compare the experimental results of different displacement. The energy depletion in tight oil reservoirs

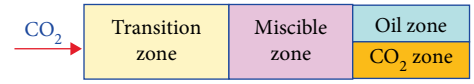

Figure 17: The zone schematic during long core displacement experiments.

is the key mechanism for fast decline of production. The energy supplement efficiency can be used for comparative investigation on the feasibility of different flooding systems in tight oil reservoir (Figure 20). The energy supplement efficiency η_p is given by

$$\eta_P = \frac{\int_0^L P_t(x)dx}{\int_0^L P_{oi}dx} \times 100\%, \tag{1}$$

where $P_t(x)$ is pressure along the sample longitude during different flooding experiments; $P_{oi}(x)$ is pressure during oil flow experiments, which is representative of reservoir pressure.

Dimensionless time is the ratio of displacement time to maximum displacement time in different flooding experiments. Figure 21 presents the relationship between energy supplement efficiency and dimensionless time. The ESE of water flooding decreases first and increases later with displacement time, which is lower than 100%. The ESE of N_2 flooding

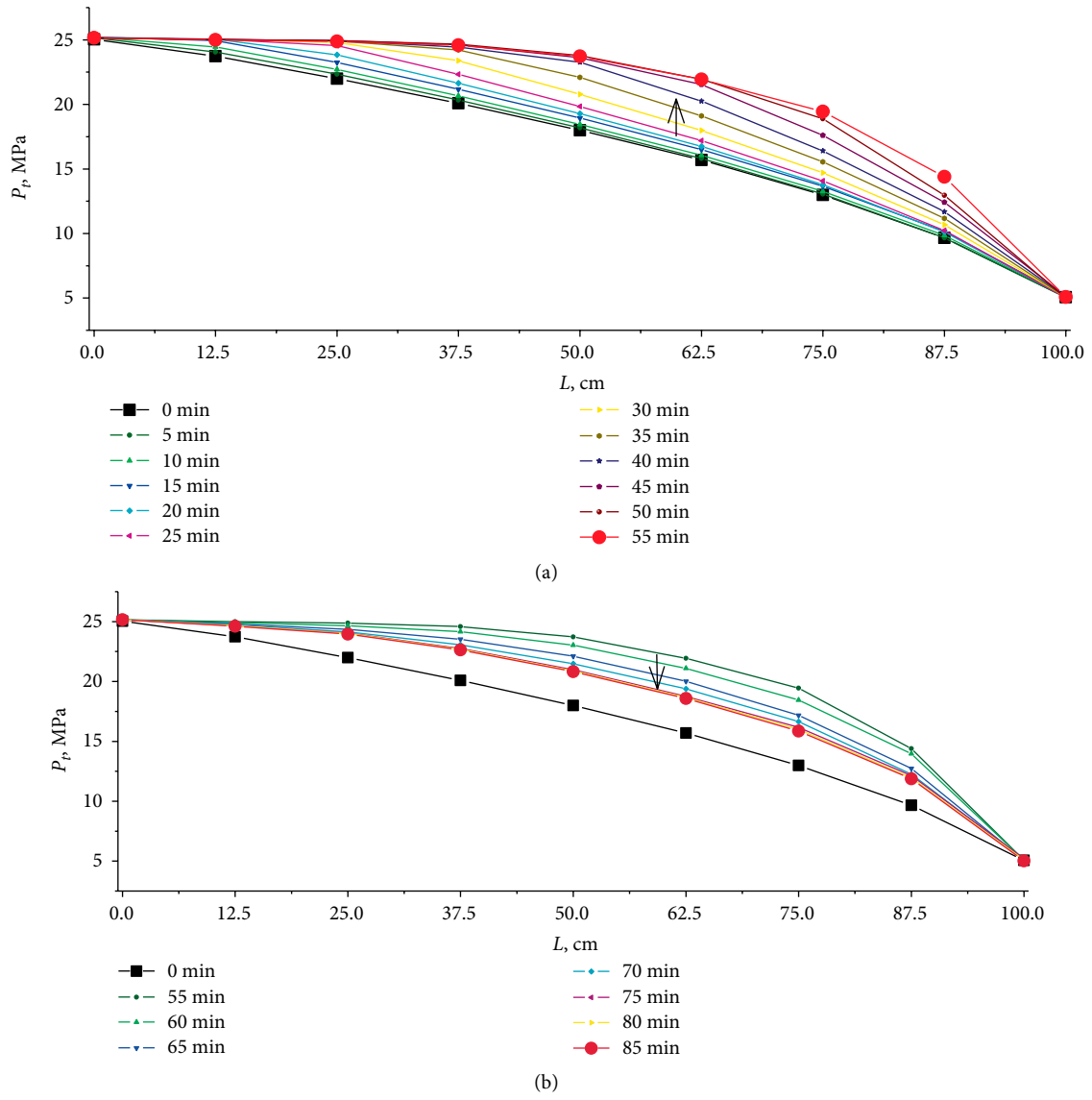

FIGURE 18: The pressure distribution in tight sandstone samples during CO_2 flooding: (a) 0–55 min and (b) 55–85 min.

rises gradually to 116%. The ESE of CO_2 flooding rises to 123% first and drops to 112% later. In contrary to water flooding, N_2 and CO_2 can increase the reservoir energy, which contributes to tight oil production. Comparatively speaking, CO_2 has better performances than N_2.

3.4.3. Oil Displacement Efficiency. The relationship between oil displacement efficiency and injected fluid volume is presented in Figure 22. The injected water is about 0.47 pore volume (PV) and the oil displacement efficiency was 43% during water flooding experiments. The injected N_2 volume is about 0.87 PV and the oil displacement efficiency was 61.9% during N_2 flooding experiments. The injected CO_2 volume is about 1.38 PV and the oil displacement efficiency was 79% during CO_2 flooding experiments. According to oil displacement efficiency, CO_2 flooding has the best performance to improve the production of tight oil, followed by N_2 and CO_2 flooding.

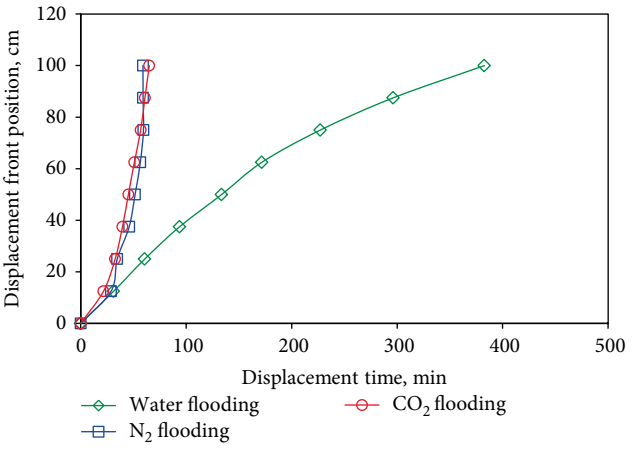

FIGURE 19: The displacement front velocity of water, CO_2 and N_2 flooding.

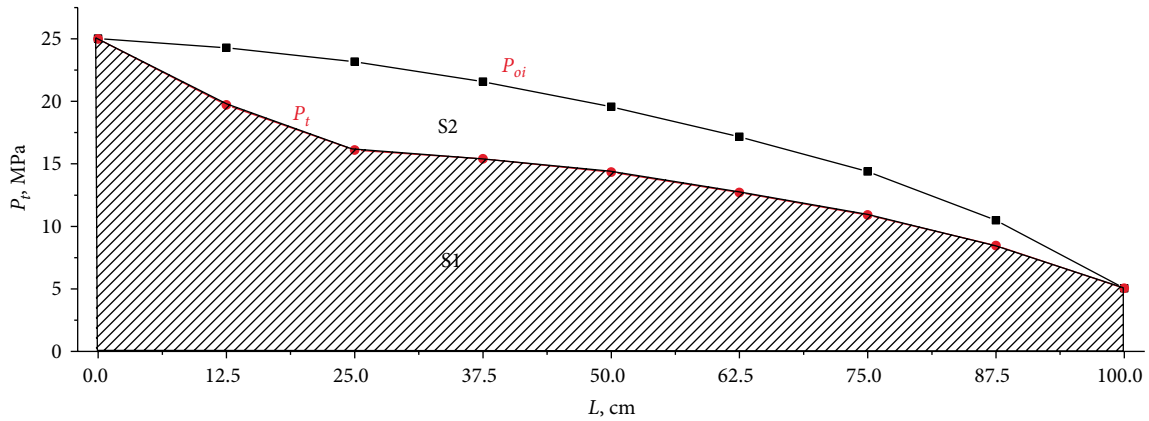

Figure 20: The energy supplement efficiency of water, CO_2 and N_2 flooding.

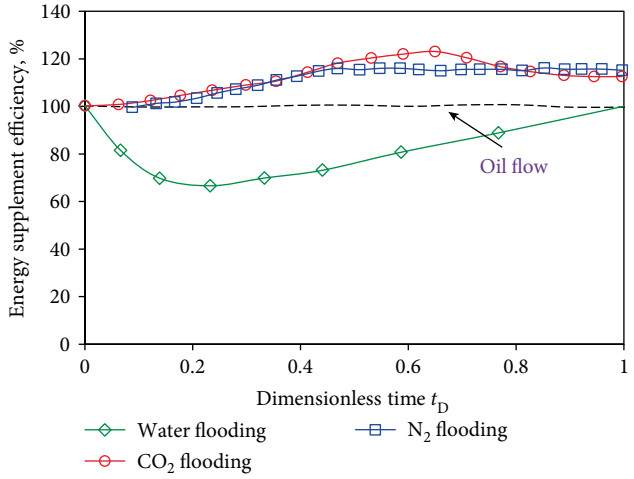

Figure 21: The energy supplement efficiency of water, CO_2 and N_2 flooding.

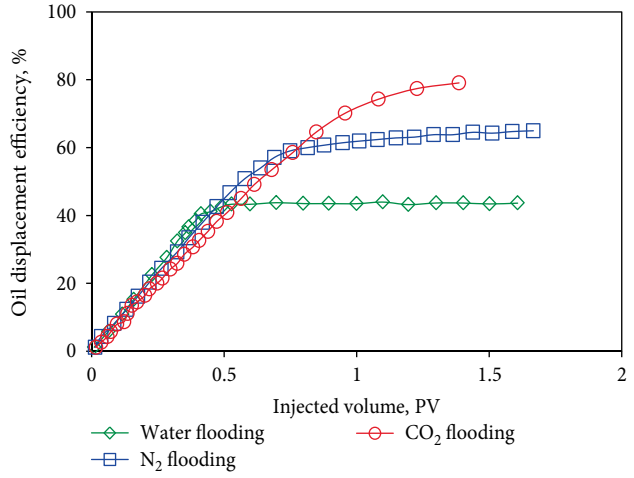

Figure 22: The oil displacement efficiency of water, CO_2 and N_2 flooding.

4. Conclusions

In this study, the water, N_2 and CO_2 flooding experiments for tight oil reservoirs are performed on the 1 m long cores. The comparative studies are based on the characteristic parameters, such as displacement front velocity, energy supplement efficiency and oil displacement efficiency. The conclusions are as follows.

(1) The SEM and NMR observations show that the oil mainly exists in the form of spots and in the micro/nano pores. Both oil spots and clay minerals have associated characteristics. The microfractures are not the storage space for oil spots, but can connect the oil spots to improve the mobility of the crude oil.

(2) The reservoir pressure of water flooding decreases first and increases later with displacement time. The reservoir pressure of N_2 flooding rises gradually over displacement time. The reservoir pressure of CO_2 flooding increases first and decreases over displacement time. In contrary to water flooding, N_2 and CO_2 can increase the reservoir energy, which contributes to tight oil production. Comparatively speaking, CO_2 has better performances than N_2.

(3) The displacement front velocities of N_2 and CO_2 are nearly equal, which are much larger that of water. However, it is more difficult to identify N_2/CO_2-water interface according to the pressure fluctuation characteristics of N_2 and CO_2 flooding. It can be explained by gas viscous fingering that results from lower viscosity of gas than that of oil.

Comparatively speaking, N_2 and CO_2 flooding is more suitable for tight oil reservoirs. However, low sweep efficiency of gas flooding should be regarded with some care. In the future work, the carbonate water that dissolves large amounts of CO_2 maybe used for oil displacement in tight oil reservoirs.

Data Availability

The datasets generated and analyzed during this study are available in the eAtlas repository.

Conflicts of Interest

The authors declare that they have no conflicts of interest.

Acknowledgments

The financial support is from National Key Research and Development Program (Grant Nos. 2018YFC0603705 and 2016YFC0600901), National Natural Science Foundation of China granted No. 11702296 and the Fundamental Research Funds for the Central Universities.

References

[1] O. Daniel Ezulike, E. Ghanbari, S. Siddiqui, and H. Dehghanpour, "Pseudo-steady state analysis in fractured tight oil reservoirs," *Journal of Petroleum Science and Engineering*, vol. 129, pp. 40–47, 2015.

[2] B. Kurtoglu, F. Rasdi, A. Salman, and H. Kazemi, "Evaluating long term flow regimes in unconventional oil reservoirs with diverse completion technology," in *SPE Unconventional Resources Conference-Canada Calgary*, 2013, SPE-167145-MS.

[3] S. An, J. Yang, L. Zhang, J. Zhao, and Y. Gao, "Influence of pore structure parameters on flow characteristics based on a digital rock and the pore network model," *Journal of Natural Gas Science and Engineering*, vol. 31, no. 4, pp. 156–163, 2016.

[4] J. D. Baihly, R. M. Altman, and I. Avlies, "Has the economic stage count been reached in the Bakken shale?" Presented at the SPE Hydrocarbon Economics and Evaluation Symposium, Calgary, 2012, SPE-159683-MS.

[5] L. Yang, H. Ge, X. Shi et al., "The effect of microstructure and rock mineralogy on water imbibition characteristics in tight reservoirs," *Journal of Natural Gas Science and Engineering*, vol. 34, pp. 1461–1471, 2016.

[6] L. Yang, H. Ge, X. Shi et al., "Experimental and numerical study on the relationship between water imbibition and salt ions diffusion in fractured shale reservoirs," *Journal of Natural Gas Science and Engineering*, vol. 38, pp. 283–297, 2017.

[7] H.-K. Ge, L. Yang, Y.-H. Shen et al., "Experimental investigation of shale imbibition capacity and the factors influencing loss of hydraulic fracturing fluids," *Petroleum Science*, vol. 12, no. 4, pp. 636–650, 2015.

[8] T. Aïfa, A. A. Zerrouki, K. Baddari, and Y. Géraud, "Magnetic susceptibility and its relation with fractures and petrophysical parameters in the tight sand oil reservoir of hamra quartzites, southwest of the hassi messaoud oil field, Algeria," *Journal of Petroleum Science and Engineering*, vol. 123, pp. 120–137, 2014.

[9] J. Xu, B. Sun, and B. Chen, "A hybrid embedded discrete fracture model for simulating tight porous media with complex fracture systems," *Journal of Petroleum Science and Engineering*, vol. 174, pp. 131–143, 2019.

[10] X. Tian, L. Cheng, R. Cao et al., "A new approach to calculate permeability stress sensitivity in tight sandstone oil reservoirs considering micro-pore-throat structure," *Journal of Petroleum Science and Engineering*, vol. 133, pp. 576–588, 2015.

[11] K. Zhang, M. E. G. Perdomo, B. K. O. Kong et al., "CO_2 near-miscible flooding for tight oil exploitation," SPE Asia Pacific Unconventional Resources Conference and Exhibition, Brisbane, Australia, 2015, SPE-176826-MS.

[12] C. Xu, P. Li, Z. Lu, L. Jianwu, and L. Detang, "Discrete fracture modeling of shale gas flow considering rock deformation," *Journal of Natural Gas Science and Engineering*, vol. 52, pp. 507–514, 2018.

[13] L. Jin, S. Hawthorne, S. Smith et al., "Improving oil recovery by use of carbon dioxide in the bakken unconventional system: a laboratory investigation," *SPE Reservoir Evaluation & Engineering*, vol. 20, no. 3, pp. 602–612, 2016.

[14] L. Yang, N. Dou, X. Lu et al., "Advances in understanding imbibition characteristics of shale using an NMR technique: a comparative study of marine and continental shale," *Journal of Geophysics and Engineering*, vol. 15, no. 4, pp. 1363–1375, 2018.

[15] Y. Yang, H. Yang, L. Tao et al., "Microscopic determination of remaining oil distribution in sandstones with different permeability scales using computed tomography scanning," *Journal of Energy Resources Technology*, vol. 141, no. 9, Article ID 092903, 2019.

[16] G. Afonja, R. G. Hughes, V. G. R. Rao, and L. Jin, "Simulation study for optimizing injected surfactant volume in a miscible carbon dioxide flood," SPETT 2012 Energy Conference and Exhibition, Port-of-Spain, Trinidad, 2012, SPE-158220-MS.

[17] T. Teramoto, H. Uematsu, K. Takabayashi, and T. Onishi, "Air injection EOR in highly water saturated light-oil reservoir," *SPE Europec/EAGE Annual Conference and Exhibition*, Vienna, Austria, 2006, SPE100215.

[18] Z. G. Tao, C. Zhu, Y. Wang, H. Manchao, and B. Zhang, "Research on stability of an open-pit mine dump with fiber optic monitoring," *Geofluids*, vol. 2018, no. 1, pp. 1–20, 2018.

[19] L. Gao, Z. Yang, and Y. Shi, "Experimental study on spontaneous imbibition chatacteristics of tight rocks," *Advances in Geo-Energy Research*, vol. 2, no. 3, pp. 292–304, 2018.

[20] T. Wan, Y. Yu, and J. J. Sheng, "Experimental and numerical study of the EOR potential in liquid-rich shales by cyclic gas injection," *Journal of Unconventional Oil Gas Resource*, vol. 12, pp. 56–67, 2015.

[21] A. Sakhaee-Pour and S. Bryant, "Gas permeability of shale," *SPE Reservoir Evaluation & Engineering*, vol. 15, no. 04, pp. 401–409, 2012.

[22] H. Singh and J. Cai, "Screening improved recovery methods in tight-oil formations by injecting and producing through fractures," *International Journal of Heat and Mass Transfer*, vol. 116, pp. 977–993, 2018.

[23] J. Zhao, J. Yao, L. Zhang, H. Sui, and M. Zhang, "Pore-scale simulation of shale gas production considering the adsorption effect," *International Journal of Heat and Mass Transfer*, vol. 103, pp. 1098–1107, 2016.

[24] F. Fu, P. Li, K. Wang, and R. Wu, "Numerical simulation of sessile droplet spreading and penetration on porous substrates," *Langmuir*, vol. 35, no. 8, pp. 2917–2924, 2019.